



**Comment on the "Discovery of high-performance thermoelectric copper chalcogenide using modified diffusion-couple high-throughput synthesis and automated histogram analysis technique" by T. Deng, T. Xing, M. K. Brod, Y. Sheng, P. Qiu, I. Veremchuk, Q. Song, T.-R. Wei, J. Yang, G. J. Snyder, Y. Grin, L. Chen and X. Shi, Energy Environ. Sci., 2020, 13, 3041**

P. Lemoine, B. Raveau, P. Boullay, E. Guilmeau

**► To cite this version:**

P. Lemoine, B. Raveau, P. Boullay, E. Guilmeau. Comment on the "Discovery of high-performance thermoelectric copper chalcogenide using modified diffusion-couple high-throughput synthesis and automated histogram analysis technique" by T. Deng, T. Xing, M. K. Brod, Y. Sheng, P. Qiu, I. Veremchuk, Q. Song, T.-R. Wei, J. Yang, G. J. Snyder, Y. Grin, L. Chen and X. Shi, Energy Environ. Sci., 2020, 13, 3041. Energy & Environmental Science, 2023, 16 (1), pp.316-320. 10.1039/d2ee01588a . hal-03969073

**HAL Id: hal-03969073**

**<https://hal.science/hal-03969073>**

Submitted on 15 Feb 2023

**HAL** is a multi-disciplinary open access archive for the deposit and dissemination of scientific research documents, whether they are published or not. The documents may come from teaching and research institutions in France or abroad, or from public or private research centers.

L'archive ouverte pluridisciplinaire **HAL**, est destinée au dépôt et à la diffusion de documents scientifiques de niveau recherche, publiés ou non, émanant des établissements d'enseignement et de recherche français ou étrangers, des laboratoires publics ou privés.



Distributed under a Creative Commons Attribution - NonCommercial 4.0 International License

**Comment on “Discovery of high-performance thermoelectric copper chalcogenide using modified diffusion-couple high-throughput synthesis and automated histogram analysis technique” by T. Deng, T. Xing, M. K. Brod, Y. Sheng, P. Qiu, I. Veremchuk, Q. Song, T-R. Wei, J. Yang, G. J. Snyder, Y. Grin, L. Chen and X. Shi, *Energy Environ. Sci.*, 2020,13, 3041-3053**

P. Lemoine,<sup>[a,c]</sup> B. Raveau,<sup>[b]</sup> P. Boullay,<sup>[b]</sup> E. Guilmeau\*<sup>[b]</sup>

<sup>[a]</sup> Univ Rennes, CNRS, ISCR – UMR 6226, F-35000 Rennes, France

<sup>[b]</sup> CRISMAT, CNRS, Normandie Univ, ENSICAEN, UNICAEN, 14000 Caen, France

Email: [emmanuel.guilmeau@ensicaen.fr](mailto:emmanuel.guilmeau@ensicaen.fr)

<sup>[c]</sup> Institut Jean Lamour, UMR 7198 CNRS – Université de Lorraine, 2 allée André Guinier-Campus ARTEM, BP 50840, 54011, Nancy Cedex, France

**Abstract.** The recent paper by Deng *et al.*<sup>1</sup> showed that a copper sulphide with Cu<sub>7</sub>Sn<sub>3</sub>S<sub>10</sub> composition is a promising thermoelectric material reaching a figure of merit  $ZT$  of 0.8 at 750 K via Cl doping. However, structural reinvestigations of Cu<sub>7</sub>Sn<sub>3</sub>S<sub>10</sub> sample (i.e. Cu<sub>2.10</sub>Sn<sub>0.90</sub>S<sub>3</sub>) prepared in the reported conditions show that the phase of interest is not tetragonal (space group  $I\bar{4}2m$ ,  $a_t = 5.4164$  Å,  $c_t = 10.832$  Å), but crystallizes in the cubic symmetry (space group  $P\bar{4}3n$ ,  $a_c = 10.832$  Å) with a composition close to Cu<sub>22</sub>Sn<sub>10</sub>S<sub>32</sub> similar to the results published by Pavan Kumar *et al.*<sup>2</sup> These observations, which indicate that the main phase around the composition Cu<sub>7</sub>Sn<sub>3</sub>S<sub>10</sub> is cubic, impose a revision of the understanding of the relationships between the structure and thermoelectric properties in this family.

In a recent article, Deng *et al.*<sup>1</sup> discovered a high performance thermoelectric with the composition Cu<sub>7</sub>Sn<sub>3</sub>S<sub>10</sub> and demonstrated that it is a promising material with ultralow thermal conductivity, moderate band gap and high electrical conductivity. A figure of merit  $ZT$  of 0.8 at 750 K was indeed reached via Cl doping. In the structural analysis of this material by powder X-ray diffraction, considering stannite-like structural models (i.e. tetragonal superstructure of the sphalerite type with the space group  $I\bar{4}2m$ ,  $a = 5.4164$  Å,  $c = 10.832$  Å), difficulties appeared in the refinement getting either chemical composition Cu<sub>39.3</sub>Sn<sub>10.7</sub>S<sub>50.0</sub> far from the nominal one Cu<sub>35</sub>Sn<sub>15</sub>S<sub>50</sub>, also confirmed by EDXS (model 1), or large spread of the atomic

displacement parameters (model 2). A further structural model was mentioned (model 3) assuming chemically improbable mixed cation/anion occupancies of the positions, but yielding expected chemical composition and reasonable values of the atomic displacement parameters. Finally, the authors decided to postpone the clarification of this issue to a separate study, and the structural model 2 was considered for the interpretation of the attractive thermoelectric properties of this material.

In posterior study of the Cu-Sn-S system, Pavan Kumar *et al.*<sup>2</sup> synthesized a low thermal conductivity degenerate semiconductor with a rather close composition,  $\text{Cu}_{22}\text{Sn}_{10}\text{S}_{32}$  (i.e.  $\text{Cu}_{2.0625}\text{Sn}_{0.9375}\text{S}_3$ ), and showed that this sulphide also exhibits attractive thermoelectric properties with a figure of merit  $ZT$  of 0.55 at 700 K via Sb for Sn substitution. For the structure solution in the tetragonal symmetry, the authors met in a first step difficulties similar to those encountered by Deng *et al.* like refined chemical composition far from the nominal one. However, they noticed that, considering the fact that the  $c$  parameter is rigorously double of the  $a$  parameter in the tetragonal structure of  $I\bar{4}2m$  space group, may imply a cubic supercell ( $a_c = 2a_t = c_t$ ).<sup>2</sup> Note that refinements reported in Deng *et al.*<sup>1</sup> article lead also to a cell parameters ratio  $c_t/a_t$  of 2. Using a combination of synchrotron powder X-ray diffraction, single crystal X-ray diffraction,  $^{119}\text{Sn}$  Mössbauer spectroscopy and transmission electron microscopy, Pavan Kumar *et al.*<sup>2</sup> demonstrated that the phase of interest crystallizes in fact in a cubic superstructure sphalerite-type with space group  $P\bar{4}3n$ , and is characterized by a semi-ordered cationic distribution: the Cu-Sn disorder being localized on one crystallographic site (see **Table 1**).

Based on the comparison of these results showing strong similitudes between  $\text{Cu}_7\text{Sn}_3\text{S}_{10}$  and  $\text{Cu}_{22}\text{Sn}_{10}\text{S}_{32}$ , we have analysed a sample provided by the group of X. Shi and prepared in the conditions reported in their paper (i.e. heat treatments at 723 K, 1223 K and 1073 K, followed by ball-milling process and SPS treatment at 923 K) to revisit the structural analysis of the materials around the composition  $\text{Cu}_7\text{Sn}_3\text{S}_{10}$  (i.e.  $\text{Cu}_{2.10}\text{Sn}_{0.90}\text{S}_3$ ). The aim of the present comment is to draw the attention on the crystal chemistry of the thermoelectric chalcogenides which requires detailed structural studies to elucidate complex order-disorder phenomena and on its impact on the understanding of their transport properties.

Rietveld refinements considering the tetragonal stannite-like (i.e. model 2) and the cubic  $\text{Cu}_{22}\text{Sn}_{10}\text{S}_{32}$  structural models, reported by Deng *et al.*<sup>1</sup> and Pavan Kumar *et al.*<sup>2</sup> respectively, have been performed on long duration (48 h) powder X-ray diffraction data collected at CRISMAT laboratory using a Bruker D8 Advance Vario A two-circle diffractometer ( $\theta$ - $2\theta$

Bragg-Brentano mode) equipped with a Ge(111) monochromator (Johansson type) and a Lynx Eye detector and a Cu X-ray tube ( $\lambda = 1.5406 \text{ \AA}$ ). Similar to the description provided by Deng *et al.*<sup>1</sup>, the Rietveld refinement considering the tetragonal stannite-like structural model ( $I\bar{4}2m$ ) gives at first sight an apparent high-quality refinement and some correct reliability factors (**Figure 1**, top panel). However, a careful analysis of the refinement reveals the presence of additional non-indexed diffraction peaks of weak intensity as clearly evidenced in the top panel of **Figure 2** with intensity in logarithmic scale. These weak intensity diffraction peaks can be indexed as superstructure diffraction reflexions in a twice larger cubic cell similar to that previously observed by Pavan Kumar *et al.*<sup>2</sup> for  $\text{Cu}_{22}\text{Sn}_{10}\text{S}_{32}$ . The reinvestigation of the crystal structure of  $\text{Cu}_7\text{Sn}_3\text{S}_{10}$  sample was then carried out with the cubic structural model reported for  $\text{Cu}_{22}\text{Sn}_{10}\text{S}_{32}$ ,<sup>2</sup> assuming that an homogeneity range with rather close compositions may exist. Rietveld refinement of the powder X-ray diffraction data considering the cubic structural model (space group  $P\bar{4}3n$ ) of the  $\text{Cu}_{22}\text{Sn}_{10}\text{S}_{32}$  phase<sup>2</sup> also provides very low reliability factors (**Figure 1**, bottom panel). Moreover, on the opposite to the tetragonal unit cell,<sup>1</sup> the cubic structural model allows to perfectly fit all of the diffraction peaks, including the weak intensity superstructure reflexions (**Figure 2**, bottom panel). Importantly, it leads to refined structural parameters and chemical composition  $\text{Cu}_{22.2(1)}\text{Sn}_{9.8(1)}\text{S}_{32}$  (**Table 1**) in fair agreement with those reported for the cubic phase  $\text{Cu}_{22}\text{Sn}_{10}\text{S}_{32}$ .<sup>2</sup> The refined composition (i.e.  $\text{Cu}_{2.08}\text{Sn}_{0.92}\text{S}_3$ ), slightly different from the nominal one  $\text{Cu}_{2.10}\text{Sn}_{0.90}\text{S}_3$ , is supported by the existence of a broad diffraction peak, detected at  $2\theta = 26.5^\circ$  (**Figure 2**), which may be assigned to a binary copper sulphide present in minor amount in the sample. Note that the refinement of the atomic parameters in the 923 K sample (**Table 1**) results in the composition  $\text{Cu}_{22.8(2)}\text{Sn}_{9.2(2)}\text{S}_{32}$ , which – in combination with the refined lattice parameter of  $10.8234(2) \text{ \AA}$  and chemical composition of  $\text{Cu}_{21.8(1)}\text{Sn}_{10.2(1)}\text{S}_{32}$  reported by Pavan Kumar *et al.*<sup>2</sup> from synchrotron PXRD data – may indicate a small homogeneity range of the cubic phase.

Moreover, it is worth pointing out that the local transmission electron microscopy analysis previously reported by Deng *et al.* (Fig. 4b in ref. 1) for “ $\text{Cu}_7\text{Sn}_3\text{S}_{10}$ ” is erroneous and incompatible with the proposed cell and space group  $I\bar{4}2m$ . Indeed, several low intensity extra reflexions in the  $[110]$  zone axis pattern, for example between the transmitted beam (000) and the reflection indexed 1-10, cannot be indexed in the  $I\bar{4}2m$  group, but on the opposite, can be indexed with the cubic cell ( $a \sim 10.8 \text{ \AA}$ ) and the space group  $P\bar{4}3n$  (**Figure 3**)

Thus, these results demonstrate without any ambiguity that the samples of composition  $\text{Cu}_7\text{Sn}_3\text{S}_{10}$  prepared in the conditions reported by Deng *et al.*<sup>1</sup> (i.e. heat treatments at 723 K,

1223 K and 1073 K, followed by ball-milling process and SPS treatment at 923 K) are biphasic and that the observed majority phase is not tetragonal with composition  $\text{Cu}_7\text{Sn}_3\text{S}_{10}$  but cubic with composition  $\text{Cu}_{22}\text{Sn}_{10}\text{S}_{32}$ .

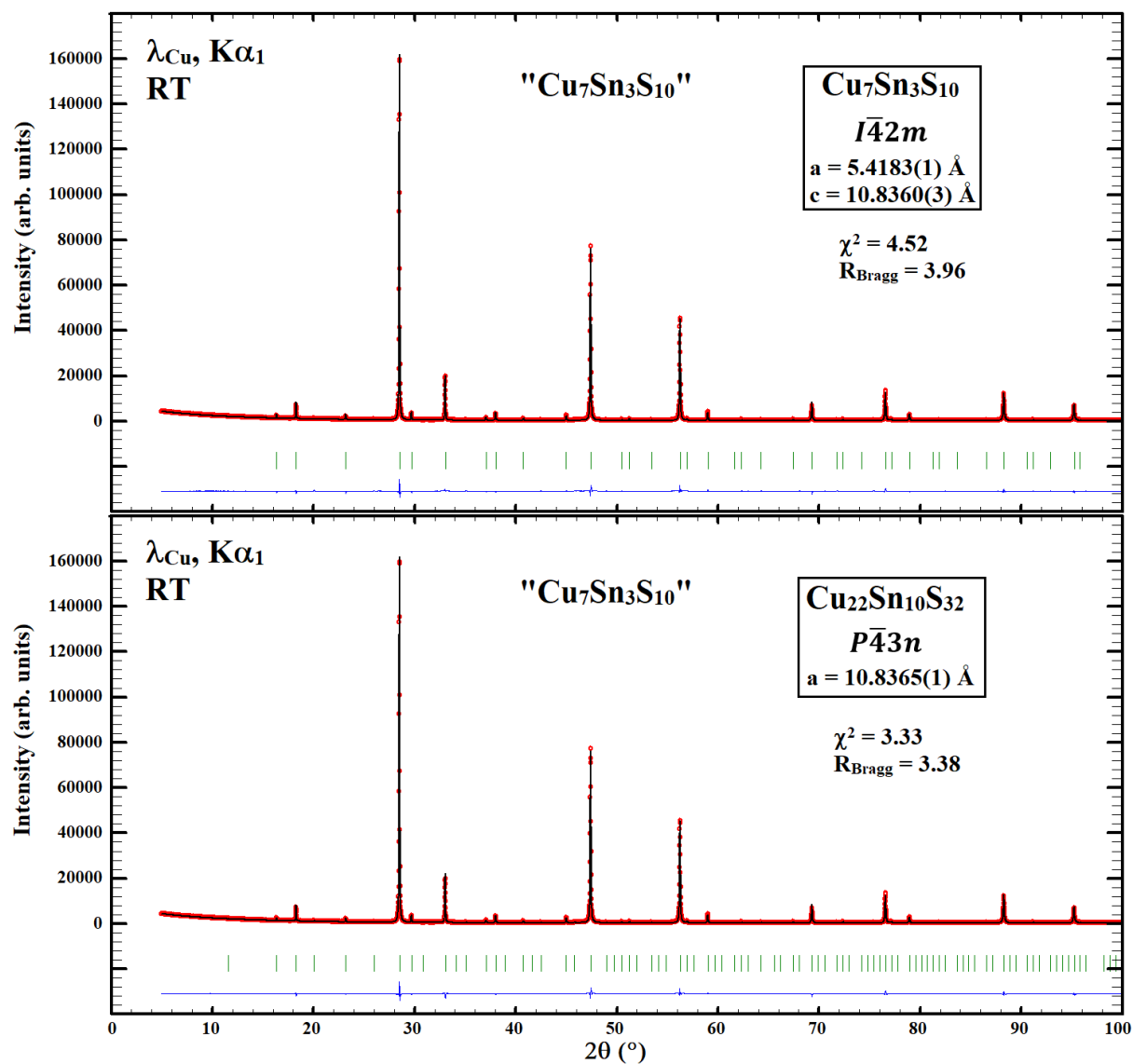


**Figure 1.** Rietveld refinement of the  $\text{Cu}_7\text{Sn}_3\text{S}_{10}$  sample considering (i) the tetragonal structural model ( $I\bar{4}2m$ ) proposed by Deng *et al.*<sup>1</sup> (top panel) and (ii) the cubic  $\text{Cu}_{22}\text{Sn}_{10}\text{S}_{32}$  structural model ( $P\bar{4}3n$ ) proposed by Pavan Kumar *et al.*<sup>2</sup> (bottom panel).

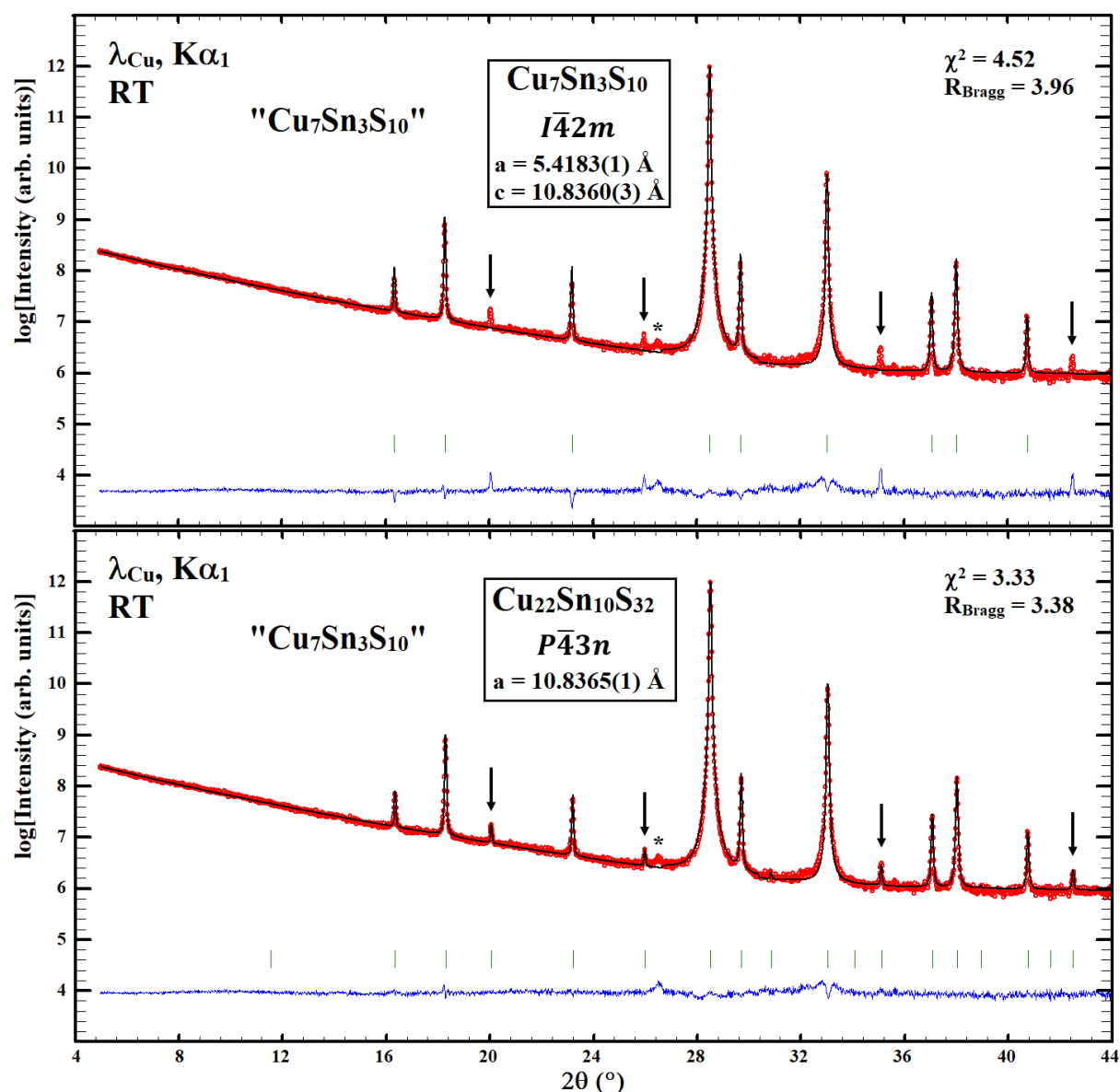


**Figure 2.** Zoom on the Rietveld refinement of the  $\text{Cu}_7\text{Sn}_3\text{S}_{10}$  sample, with intensity in logarithmic scale, considering (i) the tetragonal structural model ( $I\bar{4}2m$ ) proposed by Deng *et al.*<sup>1</sup> (top panel) and (ii) the cubic  $\text{Cu}_{22}\text{Sn}_{10}\text{S}_{32}$  structural model ( $P\bar{4}3n$ ) proposed by Pavan Kumar *et al.*<sup>2</sup> (bottom panel). \* refers to copper sulphide impurity.

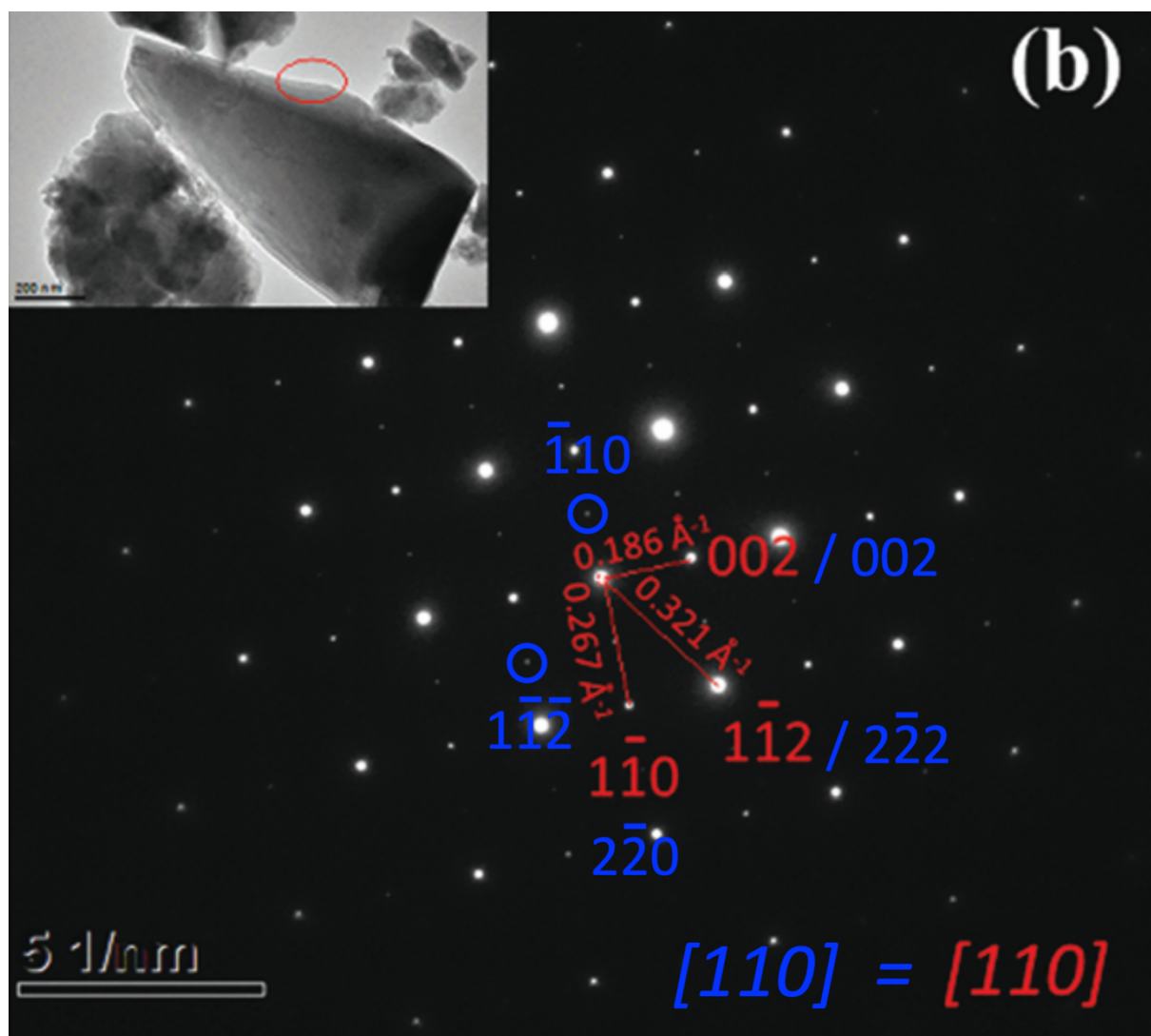


**Figure 3.** Selected area electron diffraction (SAED) pattern of the sample  $\text{Cu}_7\text{Sn}_3\text{S}_{10}$  presented by Deng *et al.*<sup>1</sup> in Figure 4. The spots with high intensity (red) were indexed by Deng *et al.* in the tetragonal cell ( $I\bar{4}2m$ ) with  $2 \times a_t = c_t$  while additional spots of weak intensity (blue) were not and cannot be indexed in this tetragonal cell. The present indexation, in blue, shows that the additional weak intensity spots are indexed in the cubic cell ( $P\bar{4}3n$ ) with  $a_c = 2 \times a_t$ .

**Table 1.** Crystallographic data of the Cu<sub>7</sub>Sn<sub>3</sub>S<sub>10</sub> sample from Rietveld refinement of the powder X-ray diffraction data considering the cubic Cu<sub>22.2(1)</sub>Sn<sub>9.8(1)</sub>S<sub>32</sub> structural model<sup>2</sup>

| $P\bar{4}3n$ , $a = 10.8365(1) \text{ \AA}$ , Cu <sub>22.2(1)</sub> Sn <sub>9.8(1)</sub> S <sub>32</sub> |      |          |          |          |                                    |                 |
|--|------|----------|----------|----------|------------------------------------|-----------------|
| Atom   | Site | x        | y        | z        | B <sub>iso</sub> (Å <sup>2</sup> ) | SOF             |
| Sn1  | 6c   | 1/4      | 1/2      | 0        | 1.28(8)                            | 1.00            |
| Cu2  | 6d   | 1/4      | 0        | 1/2      | 1.09(4)                            | 1.00            |
| Cu3  | 8e   | 0.251(1) | x        | x        | 1.23(5)                            | 1.00            |
| Cu4/Sn4  | 12f  | 0.244(1) | 0        | 0        | 0.95(7)                            | 0.68(1)/0.32(1) |
| S1   | 8e   | 0.127(1) | x        | x        | 0.78(26)                           | 1.00            |
| S2   | 24i  | 0.378(1) | 0.370(1) | 0.129(1) | 0.72(9)                            | 1.00            |

As a consequence, the crystal chemistry results, reported by Deng *et al.*,<sup>1</sup> cannot be used to explain the thermoelectric properties of the pristine Cu<sub>7</sub>Sn<sub>3</sub>S<sub>10</sub> sample. The fact that the structure of the pristine sample is cubic and not tetragonal influence significantly the interpretation previously proposed for the lattice thermal conductivity of pristine and Cl-substituted SPS-treated Cu<sub>7</sub>Sn<sub>3</sub>S<sub>10-x</sub>Cl<sub>x</sub> materials which can no more be compared on the basis of a tetragonal-cubic conversion neither on the disappearance of the distorted non-cubic framework due to the Cl-substitution.<sup>1</sup> The fact that the pristine composition exhibits a lower lattice thermal conductivity than those of disordered Cl-substituted materials remains also still quite unexpected. Indeed, Cl-substituted samples exhibit a cubic fully-disordered sphalerite structure, while the pristine composition Cu<sub>7</sub>Sn<sub>3</sub>S<sub>10</sub> (in fact cubic Cu<sub>22.2(1)</sub>Sn<sub>9.8(1)</sub>S<sub>32</sub>) has a partially ordered structure. The pristine compound should then exhibit a larger lattice thermal conductivity than the Cl-doped compounds. Full cationic disorder, induced by Cl-substitution, stoichiometry deviation or process effect, are well known to strongly enhance phonon scattering and to reduce the lattice thermal conductivity in copper-based sphalerite derivative compounds.<sup>3,4</sup> Attention must be drawn on the extremely low value of the lattice thermal conductivity of the pristine phase. A possible explanation may be in the estimation of the latter by the expression  $\kappa_L = \kappa - L\sigma T$ , where  $L$  is the Lorenz number calculated by the single parabolic band (SPB) model.<sup>5,6</sup> Unfortunately, this model is inadequate for  $L$  calculation due to the multiband nature of the valence band structure of this highly metallic degenerate semiconductor. It results in too high  $L$  values leading to a substantial underestimation of  $\kappa_L$ . This difficulty in determining the lattice contribution has been highlighted in the degenerate semiconductor Cu<sub>5</sub>Sn<sub>2</sub>S<sub>7</sub>,<sup>3,7</sup> and several thermoelectric materials, such as SnTe, for which the



presence of several electronic bands tends to lower the  $L$  values despite the strongly degenerate nature of the compound.<sup>8–11</sup>

Summarizing, our present structural investigations clearly demonstrate that the stable structure around the composition  $\text{Cu}_{2.1}\text{Sn}_{0.9}\text{S}_3$  is not tetragonal with composition  $\text{Cu}_7\text{Sn}_3\text{S}_{10}$  but cubic with space group  $P\bar{4}3n$  and the composition  $\text{Cu}_{22}\text{Sn}_{10}\text{S}_{32}$ , requiring the revision of the understanding structure-transport properties relationships of this system. Moreover, we demonstrate once again that the order-disorder phenomena in copper sulphides are very complex, and very difficult to detect. In-depth structural analyses should be then systematically performed to elucidate the subtle influence of the crystal chemistry on the electrical and thermal properties of these materials.

## Acknowledgments

We thank the group of X. Shi for having provided a sample prepared in the conditions reported in their paper (i.e. heat treatments at 723 K, 1223 K and 1073 K, followed by ball-milling process and SPS treatment at 923 K). See their experimental section.<sup>1</sup>

## References

- 1 T. Deng, T. Xing, M. K. Brod, Y. Sheng, P. Qiu, I. Veremchuk, Q. Song, T.-R. Wei, J. Yang, G. J. Snyder, Yu. Grin, L. Chen and X. Shi, *Energy Environ. Sci.*, 2020, **13**, 3041–3053.
- 2 V. Pavan Kumar, P. Lemoine, V. Carnevali, G. Guélou, O. I. Lebedev, B. Raveau, R. Al Rahal Al Orabi, M. Fornari, C. Candolfi, C. Prestipino, D. Menut, B. Malaman, J. Juraszek, K. Suekuni and E. Guilmeau, *Inorg. Chem.*, 2021, **60**, 16273–16285.
- 3 G. Guélou, V. Pavan Kumar, V. Carnevali, O. I. Lebedev, B. Raveau, C. Couder, C. Prestipino, P. Lemoine, B. Malaman, J. Juraszek, C. Candolfi, B. Lenoir, R. Al Rahal Al Orabi, M. Fornari and E. Guilmeau, *Chem. Mater.*, 2021, **33**, 9425–9438.
- 4 P. Lemoine, G. Guélou, B. Raveau and E. Guilmeau, *Angew. Chemie - Int. Ed.*, 2022, **61**, e202108686.
- 5 *Thermal Conductivity Theory, Properties, and Applications*, ed. T.M. Tritt, Kluwer Academic/Plenum Publishers, New York, 2004.

- 6 A. F. May and J. G. Snyder, in *Thermoelectrics and its energy harvesting*, ed. D. M. Rowe, CRC Press, Boca Racon, 2012, ch. 11, pp. 1-18.
- 7 V. Pavan Kumar, P. Lemoine, V. Carnevali, G. Guélou, O. I. Lebedev, P. Boullay, B. Raveau, R. Al Rahal Al Orabi, M. Fornari, C. Prestipino, D. Menut, C. Candolfi, B. Malaman, J. Juraszek and E. Guilmeau, *J. Mater. Chem. A*, 2021, **9**, 10812–10826.
- 8 R. W. McKinney, P. Gorai, V. Stevanović and E. S. Toberer, *J. Mater. Chem. A*, 2017, **5**, 17302–17311.
- 9 M. Thesberg, H. Kosina and N. Neophytou, *Phys. Rev. B*, 2017, **95**, 125206.
- 10 L. V. Prokof'eva, A. A. Shabaldin, V. A. Korchagin, S. A. Nemov and Y. I. Ravich, *Semiconductors*, 2008, **42**, 1161.
- 11 S. Misra, B. Wiendlocha, J. Tobola, F. Fesquet, A. Dauscher, B. Lenoir and C. Candolfi, *J. Mater. Chem. C*, 2020, **8**, 977–988.